

# Hydrophobic Modification on Surface of Chitin Sponges for Highly Effective Separation of Oil

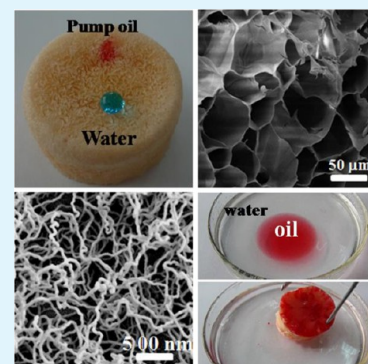
Bo Duan, Huimin Gao, Meng He, and Lina Zhang\*

Department of Chemistry, Wuhan University, Wuhan 430072, China

## S Supporting Information

**ABSTRACT:** A highly hydrophobic and oleophilic chitin sponge was synthesized, for the first time, via a freeze-dried method and then by using a thermal chemical vapor deposition of methyltrichlorosilane (MTCS) at different relative humidity. Fourier-transform infrared, energy-dispersive X-ray spectra, and scanning electron microscopy confirmed that the silanization occurred on the pore wall surface of the chitin sponge. The MTCS-coated chitin sponge had interconnected open-cell structures with the average pore size from 20 to 50  $\mu\text{m}$ , and the MTCS nanofilaments immobilized on the chitin matrix, leading to the high hydrophobicity, as a result of the existence of a solid/air composite rough surface. Cyclic compression test indicated that the hydrophobic chitin sponges exhibited excellent elasticity and high mechanical durability. The sponges could efficiently collect organics both on the surface and bottom from the water with the highest 58 times of their own weight absorption capacities through the combination of the particular wettability and great porosity. Furthermore, the biodegradation kinetics of the chitin sponge forecasted that the chitin could be completely biodegraded within 32 days by the microorganisms in the soil. This work provided a new pathway to prepare the chitin-based materials for highly effective removal of oil from water, showing potential application in the pollutant remediation field.

**KEYWORDS:** chitin sponge, surface modification, high hydrophobicity, solid/air surface, oil absorption and separation, biodegradability



## INTRODUCTION

With the development of industry and society, more environmental problems such as the water pollution resulting from oil spillage, industrial discharge of organic solvents, and heavy metal ions have emerged as a critical worldwide issue, imposing severe environmental and ecological damage.<sup>1–7</sup> To address this challenge, many efforts have been proposed for oil spill remediation, such as dispersants,<sup>8,9</sup> solidifiers,<sup>10</sup> absorbents,<sup>11–15</sup> and controlled burning. Among these techniques, the approach of using three-dimensional (3D) porous absorbents is promising and attractive because it can not only remove these chemicals but also can reclaim them.<sup>6,16–18</sup> Oil absorbents used in oil spill cleanup should meet several criteria, including high oil sorption capacity, selective oil/water separation, fast oil sorption, low density, cheap, environmentally friendly and reusability.<sup>4,19,20</sup> During recent years, a wide range of novel and advanced absorbent materials possessing hydrophobic surfaces and interconnected macroporous structure with excellent absorption performance have been developed for the recovery and separation of organic pollutants from water. Among these materials, synthetic polymers including polyurethane (PU),<sup>6,21</sup> polyvinyl-alcohol formaldehyde (PVF),<sup>22</sup> and polyvinylidene fluoride (PVDF),<sup>23</sup> and inorganic materials, such as carbon soot,<sup>24</sup> carbon nanofibril sponges,<sup>2,14</sup> vaterite particles,<sup>25</sup> carbon aerogels,<sup>26,27</sup> and graphene sponges,<sup>28</sup> have been demonstrated to be highly efficient. However, because of the high cost and complicated

fabrication procedures the large-scale fabrication of such functional materials for wide applications is very difficult.<sup>29</sup> Moreover, almost none of these materials is biodegradable, which would lead to the white pollution.<sup>30</sup> Thus, the exploitation of novel, robust, safe, and environmentally friendly materials produced from the most abundant natural polymers such as cellulose, chitin and starch, for the applications has become extremely urgent.

Recently, many researches have focused on the development of the sustainable absorbent materials based on natural products. Cellulose and chitin are the abundant nature polymers in the earth. A large amount of cellulose-based sponges have been developed as high effective oil absorbents with attractive additional properties such as renewability, good mechanical properties, low density, high porosity, and environmentally friendly.<sup>19,31–34</sup> However, to the best of our knowledge, chitin as the oil/water separation materials has been reported scarcely due to its difficult dissolution in most common solvent for further processing. In the previous work, we have successfully dissolve chitin in NaOH/urea aqueous by using freezing (–30 °C)/thawing cycles to fabricate transparent chitin solution, from which the chitin films<sup>35</sup> and microspheres<sup>36</sup> have been constructed. Moreover, the chitin-based

Received: August 12, 2014

Accepted: October 27, 2014

Published: October 27, 2014

materials have been proved to be the excellent adsorbents for many organic hazardous pollutants<sup>37,38</sup> owing to the extensive existence of the acetyl amino groups, which can trap many organic substances.

Here, we attempted to construct a chitin sponge from the chitin solution in NaOH/urea aqueous system to be employed as oil–water separation absorbents. The existence of both hydrophilic hydroxyls and acetyl amino group and hydrophobic pyranose rings on the chitin molecules, resulting in amphiphilicity of the chitin-based materials, leading to the uptake of both polar and nonpolar liquids. Chemical vapor deposition (CVD) of organosilane has become a facile process for controlling the surface chemistry to tune the hydrophobicity of hydrophilic surfaces.<sup>29,39–41</sup> Silanes with hydrolyzable group (halogen or alkoxide) can be hydrolyzed into silanols, and then condensate with each other or the hydroxyl groups on the surface of solidmatrix.<sup>32</sup> In present work, for the first time, the hydrophobic and oleophilic chitin sponges were constructed via a facile synthesis and simple thermal CVD process of organosilane on their surface. The hydrophobic chitin sponge exhibited many remarkable properties, including very low density, high porosity, good mechanical properties and excellent oil absorption performance (see Table 1). Especially,

**Table 1. Physical Properties and Si Content of the Uncoated and Coated Chitin Sponges**

sample	density (kg m <sup>-3</sup> )	porosity %	Si content relative atomic % by EDX
uncoated sponge	20.1	98.59	0
coated sponge-RH 34%	21.2	98.50	0.68
coated sponge-RH 43%	22.7	98.39	0.89
coated sponge-RH65%	24.3	98.26	1.27

the chitin sponges can be easily recycled, even after discarded in the river, lake or ocean, they could be biodegraded or digested as the forage for the fish or animal, showing the great significance for environmental protection.<sup>42</sup>

## EXPERIMENTAL SECTION

**Materials.** Chitin powder was purchased from Golden-Shell Biochemical Co. Ltd. (Zhejiang, China). The chitin powder was purified by NaOH (5 wt %) and HCl (7% HCl) aqueous to remove the residual protein and mineral as a procedure described previously.<sup>35</sup> The chitin powder was soaked in 5 wt % NaOH, 7 wt % HCl and 5 wt % NaOH for 10h, 24h and 24h in order, respectively. And after every time treatment by the NaOH (5 wt %) or HCl (7 wt %) aqueous, the chitin powder was washed with the distilled water until the pH was 7. At last, the chitin powder was dried in the oven at 60 °C for 24h. The chitin was dissolved in LiCl/DMAc with a concentration of 5% (w/v) and the weight-average molecular weight ( $M_w$ ) was determined to be  $53.4 \times 10^5$  in by dynamic light scattering (DLS, ALV/GGS-8F, ALV, Germany). All of the chemical reagents were purchased from commercial sources in China, and were of analytical-grade.

**Preparation of Chitin Hydrogels.** The chitin hydrogels were prepared according to the procedure described by our previous work.<sup>43</sup> Briefly, 22g NaOH and 8g urea were dissolved in 170g distilled water to obtain the solvent, and then 2 g chitin powder was dispersed in 98 g NaOH/urea aqueous solution (11 wt % NaOH/4% urea). After the freezing (−30 °C for 4 h)/ thawing (at room temperature) cycles for twice, transparent 2 wt % chitin solution was obtained. The chitin solution was centrifuged at 7200 rpm for 15 min at 0 °C to remove the bubbles and a few of impurities. Subsequently, 6 mL of

cross-linker of epichlorohydrin (ECH) was dropwised into 100 g of the chitin solution within 30 min and stirred at 0 °C for 1.5 h to obtain a homogeneous solution, which was then kept at 25 °C for 4 h to transform into a hydrogel. Finally, the hydrogels were immersed in distilled water for 3 days to remove any residues.

**Preparation of Hydrophobic Chitin Sponges.** The chitin hydrogel was cut into appropriate size of pieces, and precooled in a 4 °C refrigerator for 12 h to avert macroscopic fracture in the following violent freezing step. Subsequently, the precooled chitin hydrogel was frozen in a −80 °C refrigerator for 5h followed by the freeze-dried at a condenser temperature of −45 °C under vacuum (0.025 mbar) for 48h to produce the sponges. A thermal chemical vapor deposition (CVD) technique was used to modify the surface of the chitin sponges to give a hydrophobic properties to the chitin sponge. A small desiccators with chitin sponges were equilibrated for 24 h in a bigger desiccators with different relative humidity (RH 35%- 65%) at ambient temperature as shown in Figure S1 in the Supporting Information. The RH in the desiccators were controlled by the saturated solution of MgCl<sub>2</sub> (RH 34%), K<sub>2</sub>CO<sub>3</sub> (RH 43%) and NaBr (RH 65%). The coating of the chitin sponge was initiated once the 500 μL methyltrichlorosilane was transferred into the inside desiccators. The desiccators was kept at 50 °C for 12 h with the cover closed, then under vacuum at 50 °C for 1 h with the cover open. Subsequently, another 500 μL MTCS was added into the desiccators and it was kept in an oven at 50 °C for another 12 h. The surface-treated chitin sponges were kept in a vacuum oven at 50 °C under vacuum for more than 1 h to remove the residual silane and the byproduct (HCl).

**Characterization.** The mass and volume was identified to calculate the densities of the sponges. PerkinElmer Fourier-transform infrared (FT-IR) spectrometer (model 1600, Perkin–Elmer Co. USA) was used to investigate the FT-IR spectra of the samples. with the KBr-disk method. The morphologies of surface and crosssection of the chitin sponges was observed on a field emission scanning electron microscopy FESEM (SEM, SIRION TMP, FEI) with an accelerating voltage of 5 kV. The chitin sponge was sputtered with gold before observation. Two μL water was dropped onto the surface of the sponges on a Data Physics instrument (OCA20) with a dynamic mode to investigate the contact angle. The porosity was calculated by eqs 1, 2, and 3 in the Supporting Information.<sup>32</sup> Compression testing was conducted on a universal testing machine (CMT6350, Shenzhen SANS Test Machine Co., Ltd., Shenzhen, China) fitted with a 200 N load at compression rate of 10% strain min<sup>-1</sup>. The size of the tested samples for compression was cylinder (30 mm for diameter, 10 mm for height). Before the test, a 0.01N power was preloaded on the sponge.

All tests for oil removal were performed at 25 °C. The MTCS-coated sponges were weighted ( $W_0$ ), and then introduced into the mixture of various types of oils (or organic solvents) and water with 1:1 volume ratio. The volume of the absorbents was 1.5 cm × 1.5 cm × 1.5 cm cube. The weight of absorbents was monitored at decided time interval. The oil/organics swollen sponges were removed from the mixture at certain intervals, and the soaked sponges were weighed after the sponge surface was wiped with a filter paper to remove excess oil (or organic solvents)/water on the surface. The mass absorption capacity ( $Q_t$ ) at time was calculated from the mass by

$$Q_t = (W_t - W_0)/W_0 \quad (1)$$

Where  $W_0$  and  $W_t$  are the weights of the chitin sponges before and after absorption at time  $t$ , respectively. The absorption process was very fast and generally reached equilibrium within a few minutes. So, the saturated mass absorption capacity ( $Q_s$ ) was measured after the absorbents were immersed into the different oil (or organic solvents)/water mixture for 20 min. The every surface of the sponge cube was tested as the contact surface of the sponge to the oil. And the results were almost the same, indicating the different contact surface did not affect the oil adsorption performance. Then the volume-based absorption capacity was calculated by

$$V_{oil}/V_s = (m_{oil}/\rho_s)/(m_s\rho_{oil}) \quad (2)$$

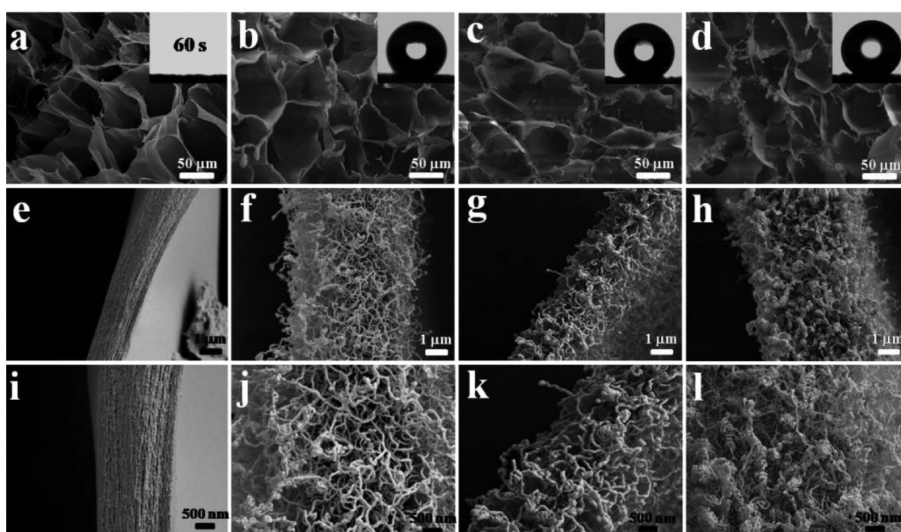
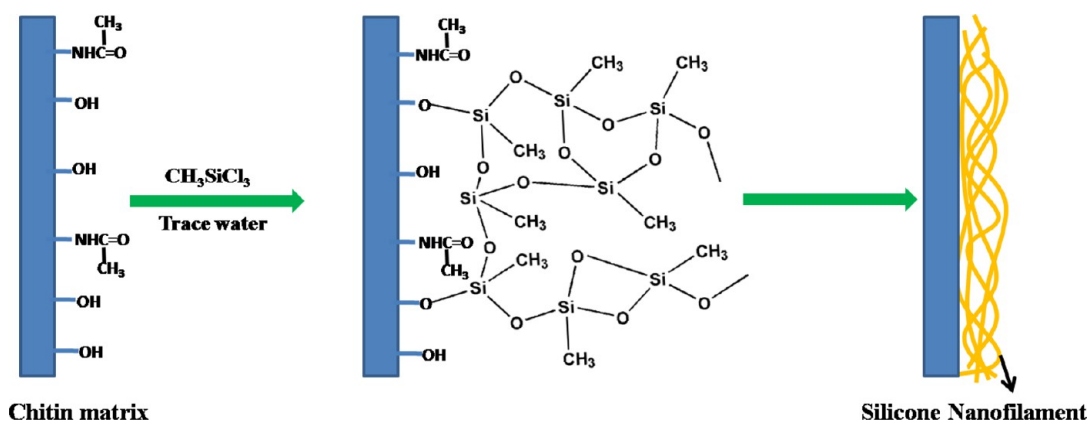


**Figure 1.** SEM images of the top surfaces of the chitin sponges: (a, e, i) uncoated chitin sponge; coated chitin sponges under RH = (b, f, j) 34%, (c, g, k) 43%, and (d, h, l) 65%, (e–l) are the magnification image of the pore wall of chitin sponge; insets in a, b, c, d corresponding to pictures taken during water contact angle measurement.

**Scheme 1. Scheme to Describe the Reaction of Methyltrichlorosilane with the Hydroxyl Groups on the Surface of Chitin Sponge**



Where  $\rho_s$  and  $\rho_{\text{oil}}$  is the density of the chitin sponges and the oils, respectively.

To study the reusability, the oil/organic swollen chitin sponges were rinsed for 10 min with 75 mL of toluene for 3 times. Subsequently, the chitin sponges were vacuum-dried at 65 °C for 8 h and then weighed.

To perform the biodegradation test, the chitin sponges (2 cm × 2 cm × 0.5 cm) enclosed in a nylon fabric (500 meshes) were buried at 8 cm depth in natural soil in a 30 L pail. The mean parameter of the soil was 23 °C, 20%, 6.8 for temperature, moisture, and pH, respectively. The degraded pieces of sponges were removed one by one, cleaned carefully with water, and then freeze-dried for 2 days. The degraded sponge samples from the burying time of 2 to 25 days were characterized with SEM and the mass change for the degradation kinetics, respectively. The 3-day intervals were chosen to investigate the weight loss of the chitin sponges.

## RESULTS AND DISCUSSION

**Structure and Hydrophobicity of the MTCS-Coated Chitin Sponge.** From the chitin solution dissolved in the NaOH/urea aqueous system at low temperature, the chitin hydrogels were fabricated according to the method previously reported in our laboratory<sup>43</sup> as shown in Figure S2 in the Supporting Information. The chitin sponges were successfully prepared from its hydrogels using freeze-drying methods. The resulting chitin sponge remained 94% of its initial volume with

the appropriate processing way. To fabricate hydrophobic sponges, we performed a simple thermal chemical vapor deposition of MTCS in a gaseous phase to modify the hydroxyl groups on the porous surface of the sponges. The structure and morphology of the chitin sponges before and after MTCS treatment was investigated by SEM measurements. Figure 1a–d shows the surface of the unmodified and modified chitin sponges. The similar highly porous microstructures with uniform pore sizes (typically 20–50 μm) displayed on the surface, confirming that the mild reactions modified with MTCS changed hardly the original structure and morphology of the chitin sponges. Interestingly, the pore on the surface of the chitin sponge was found to be oriented. It could be explained by the oriented growth of the ice crystallization from the outside of the sponge (every face of the chitin sponge) to inside. As a result, on the every surface of the chitin sponge, they exhibited the same orientation from outside to inside (see another surface in Figure S3 in the Supporting Information). After modified, a relatively denser silicone nanofilaments appeared on the surface of the pore wall of the chitin sponge (Figure 1f–h, j–l), compared with the smooth surface of the unmodified chitin sponge (Figure 1e, i). Interestingly, a relative higher humidity (RH 43%, 65%) led to the formation of organosilane spherical particles on the pore wall surface of the



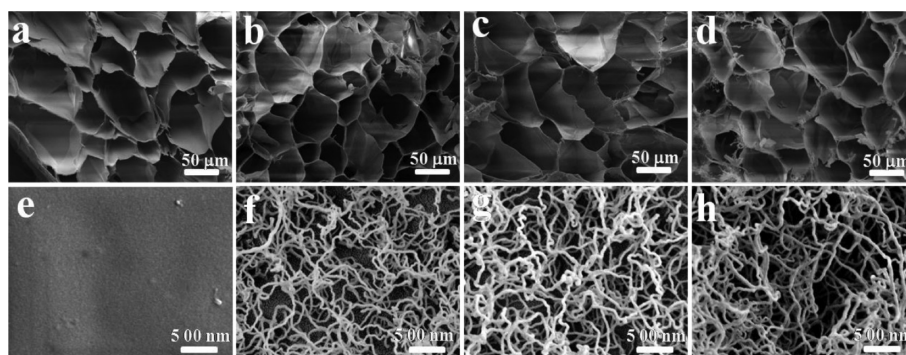


**Figure 2.** SEM images of the cross-section and enlarged view of pore wall surface of the chitin sponges: (a, e) uncoated chitin sponge; MTCS-coated chitin sponges under RH = (b, f) 34%, (c, g) 43%, and (d, h) 65%.

sponge and some much larger polysiloxane nanofiber in the holes of sponge as shown in Figure 1g, h, k, l and Figure S4 in the Supporting Information, respectively. A describing of the MTCS-coated process on the chitin sponge is proposed in Scheme 1. The formation mechanism for the coated chitin could be ascribed to the hydrolysis of MTCS, and to perform the following reaction with other silanols or the isolated hydroxyl groups on the surface of chitin sponge, leading to the remaining of the large amount of acetyl amino groups, similar to that reported in literatures.<sup>39,44</sup> The relatively large amount of water in the air led to a more rapid hydrolysis of MTCS, resulting in the formation of a string-like aggregation of the organosilane (Figure S4c, d in the Supporting Information). Thus, the silicone nanofilaments appeared on the surface of the chitin pore wall. As shown in the inset of Figure 1a, the water droplet penetrated completely into the sponge within 60 s, namely none of the corresponding static contact angle, indicating the hydrophilic surface of the pristine chitin sponge. On the contrary, the modified chitin sponges displayed remarkably higher water contact angles of  $145^\circ \pm 0.7^\circ$ ,  $146^\circ \pm 0.8^\circ$ , and  $148^\circ \pm 0.7^\circ$ , as shown in insets of Figure 1b–d, respectively. This demonstrated that the silicone nanofilaments immobilized on the surface of the chitin sponge led to the enhancement of the hydrophobicity. The SEM images of the cross-section for the chitin sponge before and after MTCS treatment are shown in Figure 2. All the sponges exhibited a highly porous structure (20–50  $\mu\text{m}$ ) with an inherent 3D-interconnected network, as shown in Figure 2a–d. Their morphology and pore size of cross-section were similar to that of the surface of the chitin sponges (see Figure 1). Noticeably, small-sized MTCS nanofilaments (with diameter of 15–50 nm) could even grow uniformly deeply and imbedded onto the pore wall surface of chitin sponge and their density and diameter increased with an increase of relative humidity, leading to the hydrophobic chitin sponges (Figure 2j, k, l and Figure S5 in the Supporting Information). Moreover, some larger nanofilaments could also be observed in the pores, as shown in Figure S6 in the Supporting Information. This result could be ascribed to (1) the rapid diffusion of the reactive precursors in the gas phase and (2) interconnected inherent porous structure of chitin sponge, enabling MTCS to permeate through the sponge skeleton. It was noted that the blocked pores inside the modified sponges could not be observed, because only the pore wall surface was modified, as shown in Figure 2. Therefore, the MTCS coated chitin sponges had high hydrophobicity and permeability. In view of the results in Figures 1 and 2, the high hydrophobicity of the modified sponges was caused by the

introduction of the hydrophobic silicone and construction of the nanofilaments on the chitin surface. Particularly, the nano- and microinterspaces between the MTCS nanofilaments could trap abundant air, resulting in a solid/air composite rough surface, leading to the high water contact angles.<sup>45–47</sup> As a result of the combination of the characteristics with the properties of the immediate transport of gas and liquid in the sponge through the open-pore 3D network structure, the MTCS coated chitin sponges would benefit the rapid uptake of oil.

**Interface Interaction between Chitin and MTCS Nanofilaments.** Energy-dispersive X-ray (EDX) spectra was also performed to investigate the silanization on the surface of the chitin sponges. Figure 3 shows the EDX spectrum of the surface of the uncoated and coated chitin sponges. The unmodified chitin sponge displayed the carbon and oxygen, and no silicon or nitrogen peaks, indicating the much lower intensity of N, compared with carbon and oxygen. After silanization, the carbon, oxygen, chlorine and silicon appeared

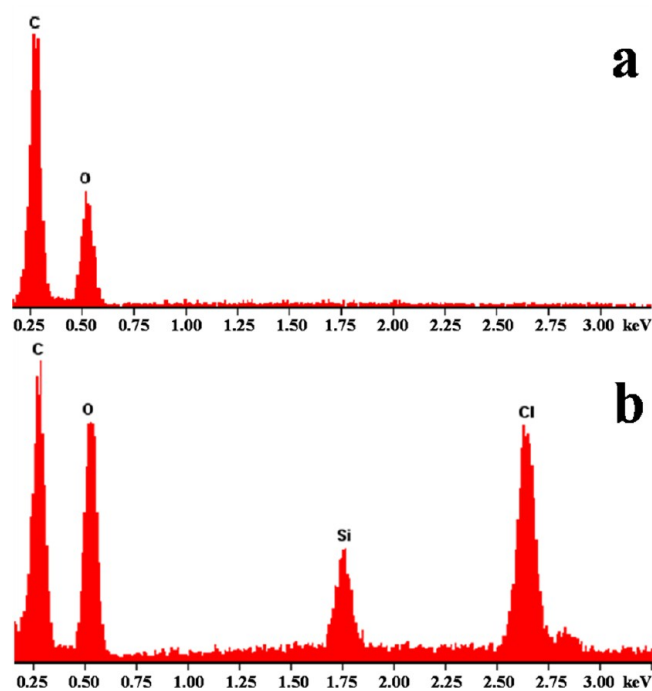


**Figure 3.** EDX spectra of the surface of the chitin sponges: (a) uncoated and (b) coated under = RH 43%.

in the EDX spectrum of the MTCS coated chitin sponge. The relative silicon atomic percentage calculated by element analysis was 0.89 (RH 43%). The silicon content increased to 1.27% with further increase of RH to 65% (Figure S7, silicon content = 0.68 for RH 34%), owing to the more hydrolysis of MTCS as shown in Table 1. Moreover, the cross-section exhibited relatively low silicon content (0.47 for RH 34%, 0.53 for RH 43%, and 0.71 for RH 65%), as a result of the relatively low density of MTCS compared with the surface as shown in Figure S8 in the Supporting Information. The silanization of the chitin sponges was further confirmed by FTIR analysis as shown in Figure 4. The amide band I and II at around 1660 and 1560

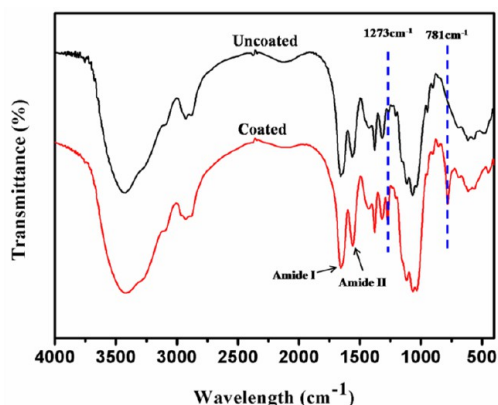


**Figure 4.** FTIR spectra of uncoated and MTCS-coated (RH 43%) chitin sponges.

$\text{cm}^{-1}$  of the chitin sponges before and after modification revealed that the acetyl amino groups were not modified. The vibrations of Si–O–Si band at  $781\text{ cm}^{-1}$  and C–Si asymmetric stretching band at  $1273\text{ cm}^{-1}$  in C–Si–O units of the MTCS-coated sponge were determined.<sup>32,48</sup> It is not hard to imagine that the mechanical stability of the porous polysiloxane coatings on the sponge could be greatly enhanced by the cross-linked Si–O–Si bond, which would be beneficial for hydrophobicity maintenance in practical application. As shown in Figure 4, the stretching vibrations of hydroxyl groups of the MTCS-coated chitin sponge was broadened and shifted to  $3419\text{ cm}^{-1}$  compared with that of the unmodified chitin sponge at  $3429\text{ cm}^{-1}$ . The results indicated that the strong interaction occurred between the hydroxyl groups of chitin and organosilane, accompanying with the covalent bonds between them (as shown in Scheme 1). Therefore, the stability of the coated organosilane on the chitin surface and the interface interaction of the two components were enhanced significantly.

For the practical application, the mechanical properties of these materials are important. Figure 5a shows the cyclic compression stress–strain curves of the MTCS-coated chitin sponges at maximum strains ( $\epsilon$ ) of 35, 50, and 65%, in which MTCS-coated chitin sponges recovered 92%, 86% and 81% of their original thickness after unloading at each strain, respectively (see Figure S9 in the Supporting Information). Hysteresis loops of the curves appeared, indicating the dissipation of mechanical energy due to friction between flowing air and the sponge skeleton. The cyclic stress–strain curves of the MTCS-coated sponges confirmed that the hydrophobic sponges could be compressed to large strains ( $\epsilon = 35\text{--}65\%$ ) at relatively low stresses (9 KPa to 26 KPa) (Figure

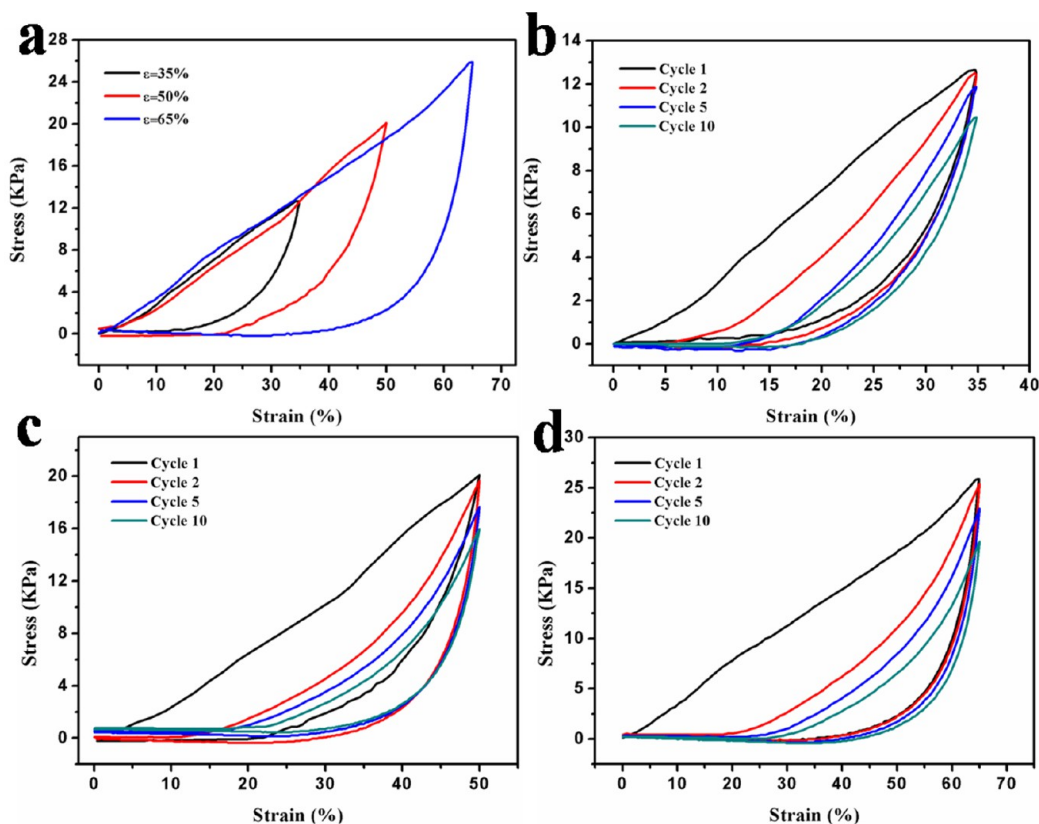


**Figure 5.** Compressive stress–strain curves of the MTCS-coated subjected to different compressive strains: (a) 35, 50, and 65%. Cyclic stress–strain curves of the chitin sponge (RH 43%) subjected to a compressive strain of (b) 35, (c) 50, and (d) 65% over 10 compression cycles.

Sb–d), indicating that it was an elastic material. Moreover, after 10 loading/unloading cycles, the shape and compressive stress of the coated chitin sponges did not undergo a violent change and maintained 71–87% (see Figure S9 in the Supporting Information) of its original thickness and around 81% of the original strength value (Figure 5b–d). This result indicated that though the modified chitin sponge could not retain their shape completely within a large deformation, it could still recover most volume (>70%) and thus kept its relatively high porosity, which would lead to its stable high absorption capacity even under the scour of organic solvent. The good compressive durability is very important for the practical application of chitin sponges.

**Surface Wettability of the Sponges.** Figure 6 shows the surface wettability of the chitin sponge. Obviously, the chitin

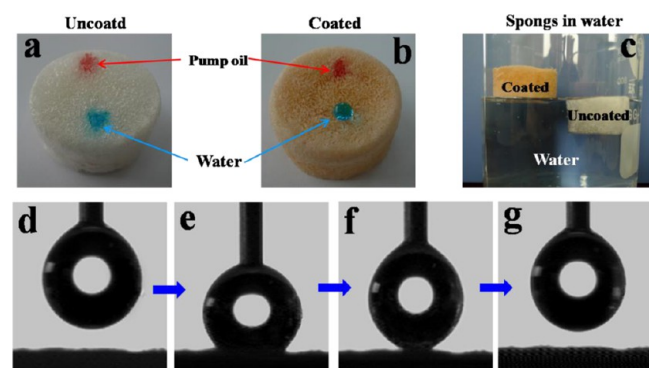


**Figure 6.** Pump oil and water were colored red (Oil Red) and blue (Neolan Blau dye) and then spotted on the surface of (a) uncoated chitin sponge and (b) coated chitin sponge (RH 43%); (c) coated chitin sponge (RH 43%) floated on water while pristine chitin sponge sank into water; (d–g) snapshots of the process of the substrates contact the water droplets.

sponge with the silicone nanofilaments displayed significantly hydrophobic surface. In Figure 6a, b, droplets of water and pump oil were successively deposited on the top surface of the unmodified and modified chitin sponges, and the pump oil immediately penetrated into the chitin strong, whereas water remained at the surface, confirming the perfect combining of the hydrophobicity and oleophilicity of the chitin sponge (Figure 6b). On the other hand, both water and pump oil could easily penetrate into the unmodified chitin sponge (Figure 6a), showing amphiphilic characteristic. After being transferred to the surface of water, the unmodified chitin sponge immediately absorbed water and sank within a short time due to its open-pore 3D porous structure and hydrophilicity. On the contrary, the MTCS-coated chitin sponge floated on water resulting from its lightweight, hydrophobicity, and water-repellent feature (Figure 6c). To further illustrate the water-repellent behavior of the hydrophobic chitin sponge, we have recorded the contact process between the substrates and water droplet, as shown in Figure 6d–g. The water droplet (2  $\mu$ L) suspending on the syringe can be hardly pulled down to the surface even when the droplet was squeezed, suggesting good hydrophobicity with a low water adhesion. The unique wettability of the coated chitin sponge toward water and oil indicated the great potential application in oil/water separation field.

**Oil Absorption Performances.** The high porosity, hydrophobicity, oleophilicity, and robust stability can make the MTCS-coated chitin sponges a wonderful candidate for the

rapid removal of various oils and organic solvents from water. Figure 7 shows the selective oil absorption properties of the

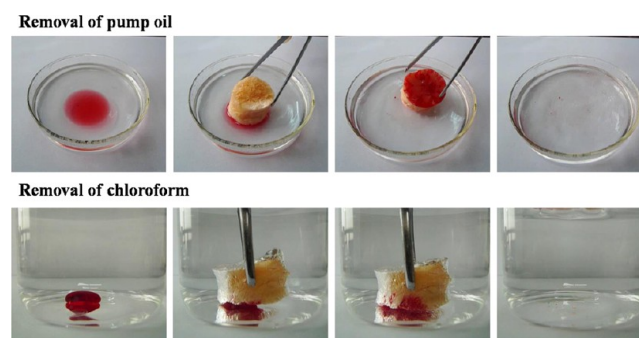


**Figure 7.** Removal of a red-colored pump oil and chloroform from surface and bottom of water with the MTCS-coated chitin sponge (RH 43%).

MTCS-coated sponge by an experiment, in which pump oil and chloroform were dropped at the surface and bottom of water, respectively. Thus, the MTCS-modified chitin sponge was introduced to contact with the organic and rapidly removed both the floated oil-red dyed pump oil and sank chloroform completely within 30 s with clear water left (Movies 1 and 2 in the Supporting Information). Moreover, its mechanical integrity was altered hardly, and the material could still be used to further remove pump oil or chloroform. The absorption performance of the MTCS-coated chitin sponges for different oils and organic solvents was investigated. Figure 8 shows the oil absorption capacity, kinetic and recyclability of the MTCS coated chitin sponges. The mass-based absorption capacities for the oils were 29 to 58 times of its own weight (Figure 8a), which were comparable with those of other polymer-based absorbents (as shown in Table S1 in the Supporting Information). Noticeably, the aerogels usually have nanoporous structure, however, our material was sponge with macroporous structure, which was more facile for their large-scale production than the aerogels. Moreover, our chitin sponges have excellent strength, biodegradability, safety, and durability. The good oil/solvent absorption capability of the MTCS-coated chitin sponge was attributed to the uniform oleophilic and hydrophobic silane nanofilaments coating on the highly porous structure surface of the chitin surface. Furthermore, the volume-based absorption capacities of the MTCS-coated chitin sponges reached up to around 90% (Figure 8b), indicating that almost all of the volume was crammed by the oil/organic. The oil absorption kinetics is another important parameter to identify the quality of absorbents. The solvents could rapidly penetrate into the interconnected pore structure of the porous absorbents and as a result, it could absorb the organic to equilibrium within a few minutes. The absorption kinetic curves of the sponges in various organic media (take the chloroform, gasoline oil, hexane, pump oil, silicon oil and toluene as the models) are shown in Figure 8c. In low viscosity organics such as chloroform, gasoline oil, hexane, and toluene, the MTCS-coated chitin sponges could absorb to equilibrium within 8 min. However, in oils with higher viscosity, such as pump oil and silicon oil, it took at least 13 min to equilibrium. Owing to the lower diffusion of the high viscosity oil molecules in the pore channel of the MTCS-coated chitin sponge, the solvation of the network and swelling in the oil was relatively slower compared with the low viscosity oil.<sup>22</sup> The results indicated that the



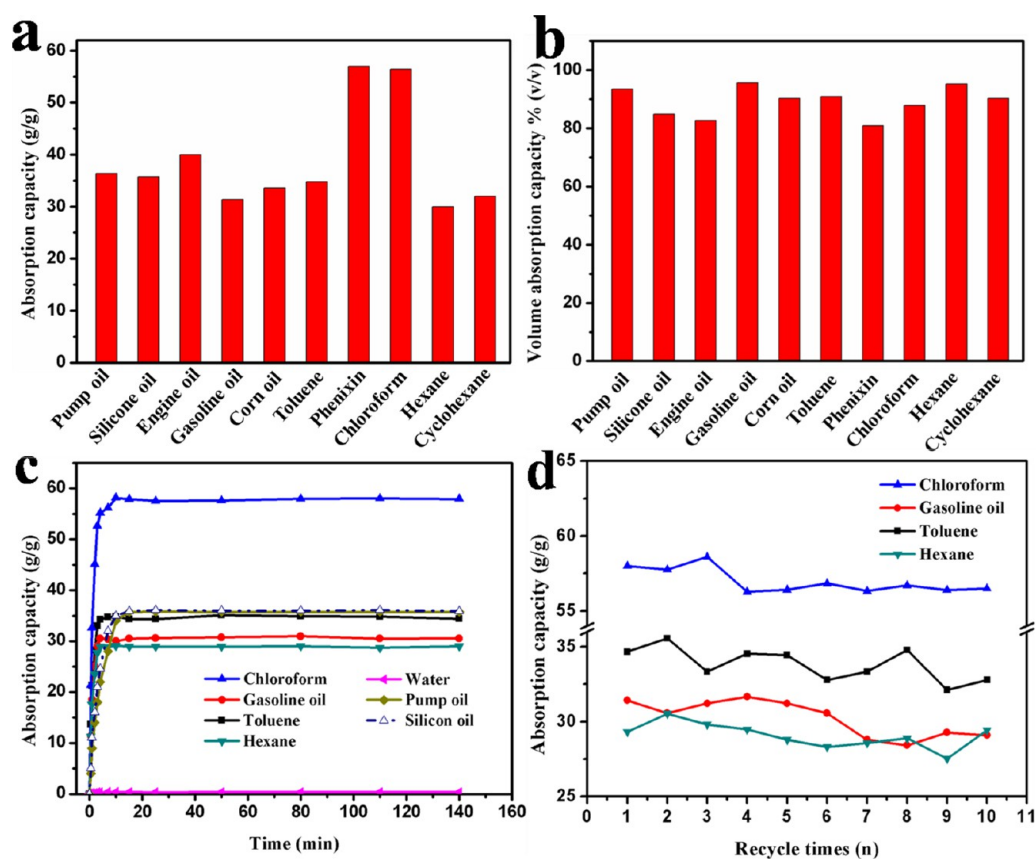


**Figure 8.** (a) Mass-based and (b) volume-based absorption capacities of the MTCS-coated chitin sponge for the measurements of oils and nonpolar solvents; (c) absorption kinetic curve and (d) repeated mass-based absorption capacity of the MTCS-coated chitin sponge (RH = 43%) for chloroform, gasoline oil, toluene, pump oil, silicon oil, and hexane, respectively.

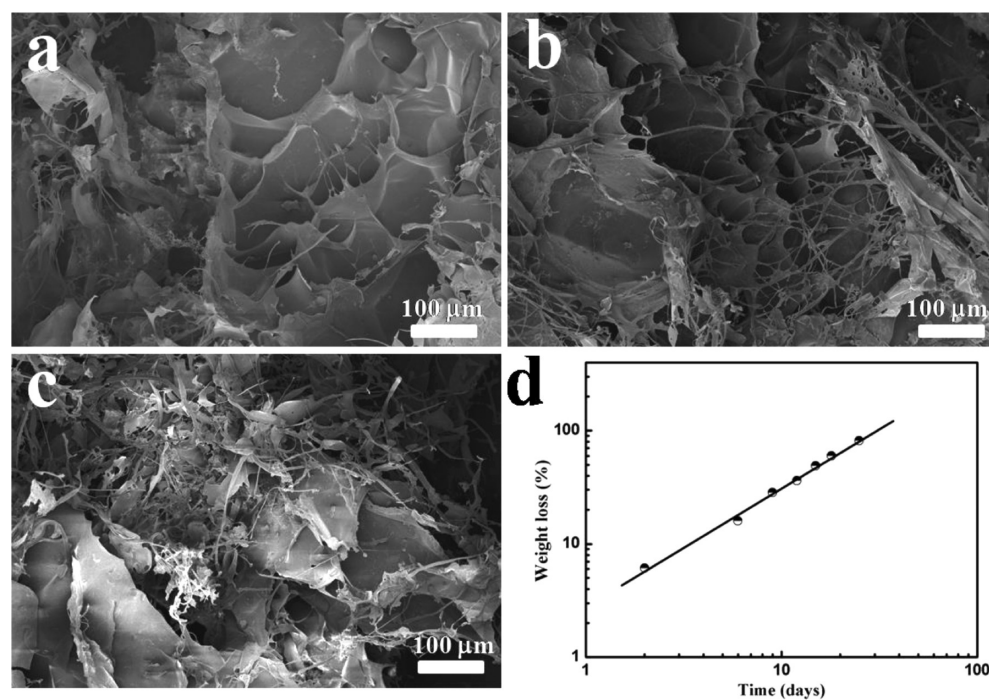


**Figure 9.** SEM images of chitin sponge surface degraded for (a) 2, (b) 6, and (c) 15 days; and (d) degradation time dependence of weight loss for the chitin sponge in soil at 23 °C.

MTCS-coated chitin sponge could rapidly and efficiently absorb the organics or oil. The water content in the MTCS-

coated chitin sponge was further analyzed by a moisture balance. The results indicated that there was extremely small

amount of water (0.3–0.4% of its own weight), confirming excellent water repellency of the MTCS-coated chitin sponge. These results proven that the MTCS-coated chitin sponge had an excellent selective absorption to many kinds of oil or organic solvents. The reusability is a significant feature for practical applications. The sponge was rinsed with toluene, subsequently vacuum-dried at 65 °C, and then recycled it for oil absorption. Even after 10 repetitions, the absorption capacities decreased slightly to 93% of its initial value, indicating a highly stable absorption performance and good recyclability (Figure 8d). Therefore, the MTCS-coated chitin sponges possessed excellent hydrophobicity, recyclability and durability. They not only could absorb and separate the nonpolar organic from the water quickly, and but also could be reused efficiently with high frequency, showing great potential in fights against the large-scale pollution of the oil or organic spillage in the river, lake, or ocean.

**Biodegradation Properties.** It is worth noting that chitin can be biodegraded in soil, and serves as a plant growth regulator to promote plant growth even after it has been discarded.<sup>49</sup> Moreover, because of its nontoxicity and digestion in many animals, they will not harm the animals even when they eat the chitin sponge by accident.<sup>50</sup> Figure 9 shows the SEM images of the biodegraded chitin sponges for (a) 2, (b) 6, and (c) 15 days. Fungal mycelia appeared rapidly on the surface of the biodegraded chitin sponge after 2 days (Figure 9a), compared with the original chitin sponge (Figure 1a). After buried in the soil for 15 days, the surface was covered with large amount of fungal mycelia, and part of the pore wall of the chitin sponge subsided, as well as the significantly biodegraded broken fragments appeared (Figure 9c). This result indicated that the chitin was attacked and digested by the microorganisms and thus was gradually biodegraded in the soil. Furthermore, it could be forecasted from the extrapolation of the plot for the biodegradable kinetics of the chitin sponge (Figure 9d) that the chitin could be completely biodegraded within 32 days in the soil. Interestingly, the MTCS-coated chitin sponge exhibited a higher degradation rate, and became into small species in 6 days, leading to the difficulty for the measurement, thus the data was not shown. The chitin was the predominant component in the modified chitin sponge, so the biodegradation of the chitin sponge could reflect that of the silane-modified one. Therefore, the chitin sponges constructed from the renewable resource via “green” process had excellent biodegradability, showing promising applications.

## CONCLUSIONS

Hydrophobic and oleophilic chitin sponges with ultralow densities (<25 kg m<sup>-3</sup>) and acetyl amino groups were created successfully via a simple and environmentally friendly freeze-drying method and then treated with a thermal chemical vapor deposition of methyltrichlorosilan. The silane nanofilaments were fixed on the pore wall surface of the chitin sponge through the strong interface interaction and covalent bonds on the chitin sponge surface. The MTCS nanofilaments immobilized on the chitin surface constructed the nano- and micro-interspaces, resulting in a solid/air composite rough surface, leading to the high hydrophobicity. The MTCS-coated chitin sponge not only rapidly (within 5 min) efficiently absorbed a wide range of oils and nonpolar organic solvents from the surface and bottom of the polluted water, but also exhibited excellent recyclability with at least 10 times. The open-cell 3D-interconnected macroporous structure, relatively high mechan-

ical properties, and oleophobic but hydrophobic surface of the MTCS-coated chitin sponges led to their highly effective removal of oil from water. The chitin sponge was safe and stable, and exhibited excellent biodegradabilities. Therefore, the coated chitin sponge materials would be important for the environmental pollutants remediation.

## ASSOCIATED CONTENT

### Supporting Information

The equation to calculate the density and porosity of the chitin sponge. The comparison of the adsorption of the chitin sponge with other adsorption materials. The device to modify the chitin sponge. Photograph of chitin hydrogel. SEM images of the surface and cross-section of the chitin sponge. Diameter distribution of the silicon nanofilaments of the MCTS-coated chitin sponge. EDX spectra of the cross-section of the coated chitin sponges. Thickness recovery (S) of silane-coated chitin sponges upon unloading from compressed. Mass-based absorption capacities of the MTCS-coated chitin sponge. Movie 1: pump oil removal process. Movie 2: chloroform removal process. This material is available free of charge via the Internet at <http://pubs.acs.org>.

## AUTHOR INFORMATION

### Corresponding Author

\*Phone: +86-27-87219274. Fax: +86-27-68754067. E-mail: [zhangln@whu.edu.cn](mailto:zhangln@whu.edu.cn) or [linazhangwhu@gmail.com](mailto:linazhangwhu@gmail.com).

### Notes

The authors declare no competing financial interest.

## ACKNOWLEDGMENTS

This work was supported by National Basic Research Program of China (973 Program, 2010CB732203), the Major Program of National Natural Science Foundation of China (21334005) and the National Natural Science Foundation of China (20874079).

## REFERENCES

- (1) Ruan, C.; Ai, K.; Li, X.; Lu, L. A Superhydrophobic Sponge with Excellent Absorbency and Flame Retardancy. *Angew. Chem., Int. Ed.* **2014**, *53*, 5556–5560.
- (2) Wu, Z.-Y.; Li, C.; Liang, H.-W.; Chen, J.-F.; Yu, S.-H. Ultralight, Flexible, and Fire-Resistant Carbon Nanofiber Aerogels from Bacterial Cellulose. *Angew. Chem., Int. Ed.* **2013**, *52*, 2925–2929.
- (3) Kansal, S. K.; Kumari, A. Potential of *M. oleifera* for the Treatment of Water and Wastewater. *Chem. Rev.* **2014**, *114*, 4993–5010.
- (4) Wang, F.; Lei, S.; Xue, M.; Ou, J.; Li, W. In Situ Separation and Collection of Oil from Water Surface via a Novel Superoleophilic and Superhydrophobic Oil Containment Boom. *Langmuir* **2014**, *30*, 1281–1289.
- (5) Brown, P. S.; Atkinson, O. D. L. A.; Badyal, J. P. S. Ultrafast Oleophobic–Hydrophilic Switching Surfaces for Antifogging, Self-Cleaning, and Oil–Water Separation. *ACS Appl. Mater. Interfaces* **2014**, *6*, 7504–7511.
- (6) Liu, Y.; Ma, J.; Wu, T.; Wang, X.; Huang, G.; Liu, Y.; Qiu, H.; Li, Y.; Wang, W.; Gao, J. Cost-Effective Reduced Graphene Oxide-Coated Polyurethane Sponge As a Highly Efficient and Reusable Oil-Absorbent. *ACS Appl. Mater. Interfaces* **2013**, *5*, 10018–10026.
- (7) Cao, Y.; Liu, N.; Fu, C.; Li, K.; Tao, L.; Feng, L.; Wei, Y. Thermo and pH Dual-Responsive Materials for Controllable Oil/Water Separation. *ACS Appl. Mater. Interfaces* **2014**, *6*, 2026–2030.
- (8) Kujawinski, E. B.; Kido Soule, M. C.; Valentine, D. L.; Boysen, A. K.; Longnecker, K.; Redmond, M. C. Fate of Dispersants Associated



with the Deepwater Horizon Oil Spill. *Environ. Sci. Technol.* **2011**, *45*, 1298–1306.

(9) Li, S.; Li, N.; Yang, S.; Liu, F.; Zhou, J. The Synthesis of a Novel Magnetic Demulsifier and its Application for the Demulsification of Oil-charged Industrial Wastewaters. *J. Mater. Chem. A* **2014**, *2*, 94–99.

(10) Jadhav, S. R.; Vemula, P. K.; Kumar, R.; Raghavan, S. R.; John, G. Sugar-Derived Phase-Selective Molecular Gelators as Model Solidifiers for Oil Spills. *Angew. Chem., Int. Ed.* **2010**, *49*, 7695–7698.

(11) Zhu, H.; Qiu, S.; Jiang, W.; Wu, D.; Zhang, C. Evaluation of Electrospun Polyvinyl Chloride/Polystyrene Fibers As Sorbent Materials for Oil Spill Cleanup. *Environ. Sci. Technol.* **2011**, *45*, 4527–4531.

(12) Wang, C.-F.; Tzeng, F.-S.; Chen, H.-G.; Chang, C.-J. Ultraviolet-Durable Superhydrophobic Zinc Oxide-Coated Mesh Films for Surface and Underwater–Oil Capture and Transportation. *Langmuir* **2012**, *28*, 10015–10019.

(13) Chu, Y.; Pan, Q. Three-Dimensionally Macroporous Fe/C Nanocomposites As Highly Selective Oil-Absorption Materials. *ACS Appl. Mater. Interfaces* **2012**, *4*, 2420–2425.

(14) Liu, H.; Cao, C.-Y.; Wei, F.-F.; Huang, P.-P.; Sun, Y.-B.; Jiang, L.; Song, W.-G. Flexible Macroporous Carbon Nanofiber Film with High Oil Adsorption Capacity. *J. Mater. Chem. A* **2014**, *2*, 3557–3562.

(15) Hu, Y.; Liu, X.; Zou, J.; Gu, T.; Chai, W.; Li, H. Graphite/Isobutylene-isoprene Rubber Highly Porous Cryogels as New Sorbents for Oil Spills and Organic Liquids. *ACS Appl. Mater. Interfaces* **2013**, *5*, 7737–7742.

(16) Wang, B.; Karthikeyan, R.; Lu, X.-Y.; Xuan, J.; Leung, M. K. H. Hollow Carbon Fibers Derived from Natural Cotton as Effective Sorbents for Oil Spill Cleanup. *Ind. Eng. Chem. Res.* **2013**, *52*, 18251–18261.

(17) Wang, F.; Lei, S.; Xue, M.; Ou, J.; Li, C.; Li, W. Superhydrophobic and Superoleophilic Miniature Device for the Collection of Oils from Water Surfaces. *J. Phys. Chem. C* **2014**, *118*, 6344–6351.

(18) Wang, C.-F.; Lin, S.-J. Robust Superhydrophobic/Superoleophilic Sponge for Effective Continuous Absorption and Expulsion of Oil Pollutants from Water. *ACS Appl. Mater. Interfaces* **2013**, *5*, 8861–8864.

(19) Zhang, Z.; Sèbe, G.; Rentsch, D.; Zimmermann, T.; Tingaut, P. Ultralightweight and Flexible Silylated Nanocellulose Sponges for the Selective Removal of Oil from Water. *Chem. Mater.* **2014**, *26*, 2659–2668.

(20) Zhou, X.; Zhang, Z.; Xu, X.; Men, X.; Zhu, X. Facile Fabrication of Superhydrophobic Sponge with Selective Absorption and Collection of Oil from Water. *Ind. Eng. Chem. Res.* **2013**, *52*, 9411–9416.

(21) Zhu, Q.; Pan, Q. Mussel-Inspired Direct Immobilization of Nanoparticles and Application for Oil–Water Separation. *ACS Nano* **2014**, *8*, 1402–1409.

(22) Pan, Y.; Shi, K.; Peng, C.; Wang, W.; Liu, Z.; Ji, X. Evaluation of Hydrophobic Polyvinyl-Alcohol Formaldehyde Sponges As Absorbents for Oil Spill. *ACS Appl. Mater. Interfaces* **2014**, *6*, 8651–8659.

(23) Li, R.; Chen, C.; Li, J.; Xu, L.; Xiao, G.; Yan, D. A Facile Approach to Superhydrophobic and Superoleophilic Graphene/polymer Aerogels. *J. Mater. Chem. A* **2014**, *2*, 3057–3064.

(24) Gao, Y.; Zhou, Y. S.; Xiong, W.; Wang, M.; Fan, L.; Rabiee-Golgir, H.; Jiang, L.; Hou, W.; Huang, X.; Jiang, L.; Silvain, J.-F.; Lu, Y. F. Highly Efficient and Recyclable Carbon Soot Sponge for Oil Cleanup. *ACS Appl. Mater. Interfaces* **2014**, *6*, 5924–5929.

(25) Sarkar, A.; Mahapatra, S. Novel Hydrophobic Vaterite Particles for Oil Removal and Recovery. *J. Mater. Chem. A* **2014**, *2*, 3808–3818.

(26) Yang, Y.; Tong, Z.; Ngai, T.; Wang, C. Nitrogen-Rich and Fire-Resistant Carbon Aerogels for the Removal of Oil Contaminants from Water. *ACS Appl. Mater. Interfaces* **2014**, *6*, 6351–6360.

(27) Li, Y.-Q.; Samad, Y. A.; Polychronopoulou, K.; Alhassan, S. M.; Liao, K. Carbon Aerogel from Winter Melon for Highly Efficient and Recyclable Oils and Organic Solvents Absorption. *ACS Sustainable Chem. Eng.* **2014**, *2*, 1492–1497.

(28) Wu, C.; Huang, X.; Wu, X.; Qian, R.; Jiang, P. Mechanically Flexible and Multifunctional Polymer-Based Graphene Foams for Elastic Conductors and Oil-Water Separators. *Adv. Mater.* **2013**, *25*, 5658–5662.

(29) Zhang, J.; Seeger, S. Polyester Materials with Superwetting Silicone Nanofilaments for Oil/Water Separation and Selective Oil Absorption. *Adv. Funct. Mater.* **2011**, *21*, 4699–4704.

(30) Lin, X.; Li, Y.; Chen, Z.; Zhang, C.; Luo, X.; Du, X.; Huang, Y. Synthesis, Characterization and Electrospinning of New Thermoplastic Carboxymethyl Cellulose (TCMC). *Chem. Eng. J.* **2013**, *215*–216, 709–720.

(31) Jiang, F.; Hsieh, Y.-L. Amphiphilic Superabsorbent Cellulose Nanofibril Aerogels. *J. Mater. Chem. A* **2014**, *2*, 6337–6342.

(32) Zheng, Q.; Cai, Z.; Gong, S. Green synthesis of Polyvinyl Alcohol (PVA)-Cellulose Nanofibril (CNF) Hybrid Aerogels and Their Use as Superabsorbents. *J. Mater. Chem. A* **2014**, *2*, 3110–3118.

(33) Korhonen, J. T.; Kettunen, M.; Ras, R. H. A.; Ikkala, O. Hydrophobic Nanocellulose Aerogels as Floating, Sustainable, Reusable, and Recyclable Oil Absorbents. *ACS Appl. Mater. Interfaces* **2011**, *3*, 1813–1816.

(34) Javadi, A.; Zheng, Q.; Payen, F.; Javadi, A.; Altin, Y.; Cai, Z.; Sabo, R.; Gong, S. Polyvinyl Alcohol-Cellulose Nanofibrils-Graphene Oxide Hybrid Organic Aerogels. *ACS Appl. Mater. Interfaces* **2013**, *5*, 5969–5975.

(35) Duan, B.; Chang, C.; Ding, B.; Cai, J.; Xu, M.; Feng, S.; Ren, J.; Shi, X.; Du, Y.; Zhang, L. High Strength Films with Gas-barrier Fabricated from Chitin Solution Dissolved at Low Temperature. *J. Mater. Chem. A* **2013**, *1*, 1867–1874.

(36) Duan, B.; Liu, F.; He, M.; Zhang, L. Ag-Fe<sub>3</sub>O<sub>4</sub> Nanocomposites@Chitin Microspheres Constructed by In Situ One-Pot Synthesis for Rapid Hydrogenation Catalysis. *Green Chem.* **2014**, *16*, 2835–2845.

(37) Tang, H.; Zhou, W. J.; Zhang, L. N. Adsorption Isotherms and Kinetics Studies of Malachite Green on Chitin Hydrogels. *J. Hazard Mater.* **2012**, *209*, 218–225.

(38) Crini, G. Recent Developments in Polysaccharide-based Materials Used as Adsorbents in Wastewater Treatment. *Prog. Polym. Sci.* **2005**, *30*, 38–70.

(39) Artus, G. R. J.; Jung, S.; Zimmermann, J.; Gautschi, H. P.; Marquardt, K.; Seeger, S. Silicone Nanofilaments and Their Application as Superhydrophobic Coatings. *Adv. Mater.* **2006**, *18*, 2758–2762.

(40) Jin, M.; Wang, J.; Yao, X.; Liao, M.; Zhao, Y.; Jiang, L. Underwater Oil Capture by a Three-Dimensional Network Architected Organosilane Surface. *Adv. Mater.* **2011**, *23*, 2861–2864.

(41) Glavan, A. C.; Martinez, R. V.; Subramaniam, A. B.; Yoon, H. J.; Nunes, R. M. D.; Lange, H.; Thuo, M. M.; Whitesides, G. M. Omniphobic “RF Paper” Produced by Silanization of Paper with Fluoroalkyltrichlorosilanes. *Adv. Funct. Mater.* **2014**, *24*, 60–70.

(42) Hirano, S.; Itakura, C.; Seino, H.; Akiyama, Y.; Nonaka, I.; Kanbara, N.; Kawakami, T. Chitosan as an Ingredient for Domestic Animal Feeds. *J. Agric. Food Chem.* **1990**, *38*, 1214–1217.

(43) Chang, C.; Chen, S.; Zhang, L. Novel Hydrogels Prepared via Direct Dissolution of Chitin at Low Temperature: Structure and Biocompatibility. *J. Mater. Chem.* **2011**, *21*, 3865–3871.

(44) Gao, L.; McCarthy, T. J. A Perfectly Hydrophobic Surface ( $\theta_A/\theta_R = 180^\circ/180^\circ$ ). *J. Am. Chem. Soc.* **2006**, *128*, 9052–9053.

(45) Crick, C. R.; Parkin, I. P. Preparation and Characterisation of Super-Hydrophobic Surfaces. *Chem.—Eur. J.* **2010**, *16*, 3568–3588.

(46) He, M.; Kwok, R. T. K.; Wang, Z.; Duan, B.; Tang, B. Z.; Zhang, L. Hair-Inspired Crystal Growth of HOA in Cavities of Cellulose Matrix via Hydrophobic–Hydrophilic Interface Interaction. *ACS Appl. Mater. Interfaces* **2014**, *6*, 9508–9516.

(47) He, M.; Xu, M.; Zhang, L. Controllable Stearic Acid Crystal Induced High Hydrophobicity on Cellulose Film Surface. *ACS Appl. Mater. Interfaces* **2013**, *5*, 585–591.

(48) Zhu, Q.; Chu, Y.; Wang, Z.; Chen, N.; Lin, L.; Liu, F.; Pan, Q. Robust Superhydrophobic Polyurethane Sponge As a Highly Reusable Oil-absorption Material. *J. Mater. Chem. A* **2013**, *1*, 5386–5393.

- (49) Tang, H.; Zhang, L.; Hu, L.; Zhang, L. Application of Chitin Hydrogels for Seed Germination, Seedling Growth of Rapeseed. *J. Plant Growth Regul* **2014**, *33*, 195–201.
- (50) Fagbenro, O. A.; Bello-Olusoji, O. A. Preparation, Nutrient Composition and Digestibility of Fermented Shrimp Head Silage. *Food Chem.* **1997**, *60*, 489–493.